# Study of Ethanol–Lysozyme Interactions Using Neutron Diffraction

M. S. Lehmann,* S. A. Mason, and G. J. McIntyre

*Institut Laue-Langevin, 38042 Grenoble Cedex, France*

*Received March 8, 1985*

ABSTRACT: Single-crystal neutron diffraction has been used to observe the interactions between deuterated ethanol ($CD_3CD_2OH$) and lysozyme in triclinic crystals of hen egg white lysozyme soaked in 25% (v/v) ethanol solutions. A total of 6047 observed reflections to a resolution of 2 Å were used, and 13 possible ethanol sites were identified. The three highest occupied sites are close to locations for bromoethanol found in an earlier study by Yonath et al. [Yonath, A., Podjarny, A., Honig, B., Traub, W., Sielecki, A., Herzberg, O., & Moult, J. (1978) *Biophys. Struct. Mech. 4*, 27–36]. Structure refinements including a model for the flat solvent lead to a final crystallographic agreement factor of 0.097. Comparison with earlier neutron studies on triclinic lysozyme showed that neither the molecular structure nor the thermal motions were affected significantly by the ethanol. A detailed analysis of the ethanol–lysozyme contacts showed 61% of these to be with hydrophobic sites, in agreement with the dominant hydrophobic nature of ethanol. This, together with the fact that the molecular structure of lysozyme is not perturbed, suggests a model for denaturation of lysozyme by alcohol, which proceeds via a dehydration of the protein at high alcohol concentration.

Much of the biological activity of proteins takes place in contact with aqueous solutions, and the interactions of the macromolecule with water and other small molecules have therefore been studied extensively. In recent neutron small-angle scattering studies of proteins in ethanol–water solutions and glycerol–water solutions (Lehmann & Zaccaï, 1982), it was found that the regions near the molecule from which ethanol and glycerol were excluded were quite different for the two molecules. For glycerol, the region containing only water corresponded to 0.23 ± 0.05 g of water/g of protein, whereas for ethanol the value was −0.07 ± 0.05. The protein surface therefore seemed to be equally accessible to ethanol and water for the concentrations studied, which were limited to 30% (v/v) ethanol. From the small-angle scattering study, as from the majority of other studies of solvent–protein interactions, one obtains no detailed geometrical information. It therefore seemed of interest to carry these studies further and to determine from a structure analysis of a protein crystal soaked in an ethanol solution the possible locations of ethanol.

Hen egg white lysozyme was used for the study since large triclinic crystals can easily be grown, and the structure is well-known both from X-ray and neutron diffraction analysis (Hodsdon et al., 1975; Mason et al., 1984). Furthermore, neutron small-angle scattering studies (M. S. Lehmann, unpublished results) have shown that the behavior of lysozyme toward ethanol is similar to the behavior found in previous studies on other proteins as mentioned above.

The single-crystal study was done with neutron diffraction techniques as it is possible with the right choice of deuterated and nondeuterated molecules to accentuate the signal from the ethanol molecules. The scattering density of $CD_3CD_2OH$ is $0.050 \times 10^{-12}$ cm/Å$^3$, whereas the scattering density for the nondeuterated lysozyme is $0.019 \times 10^{-12}$ cm/Å$^3$ [scattering lengths for the individual species are $b_H = -0.374$, $b_D = 0.667$, $b_C = 0.665$, $b_N = 0.921$, $b_O = 0.581$, and $b_S = 0.285$, all in units of $10^{-12}$ cm (Koester & Rauch, 1981)]. Neutron diffraction analysis should thus be more effective than X-ray analysis, where the corresponding values are 0.27 electron/Å$^3$ for ethanol and 0.43 electron/Å$^3$ for protein. Moreover, in the neutron case the scattering from the disordered water is approximately zero, whereas the X-ray scattering densities for ethanol and water are nearly identical and about 60% of the scattering density of the protein. Hence, the neutron diffraction analysis on a nondeuterated protein with deuterated ethanol should be an optimal way of locating the bound ethanol molecules.

## Experimental Procedures

*Crystal Growth and Data Recording.* Large triclinic single crystals of hen egg white lysozyme were grown in 0.05 M acetate buffer (pH 4.6) containing 2% $NaNO_3$ and 0.5% protein. Ethanol 99.3% enriched in deuterium came from Service des Molécules Marquées, CEA, Gif-sur-Yvette (lot 6-79). The $CD_3CD_2OD$ was slowly added to the mother liquor over a period of 10 days until a volume concentration of ethanol of 25% was reached, and the diffraction measurements were started 20 days later. The crystal used for the measurement had a volume of 12.8 mm$^3$, and the approximate maximum dimensions along the three axial directions were 3.1, 4.7, and 2.0 mm. It was mounted in a cryorefrigerator (Allibon et al., 1981) on the diffractometer D8 of the Institut Laue-Langevin, and the measurement was carried out at 280 K, the same temperature at which an earlier experiment on nondeuterated native lysozyme, H-TLY (G. J. McIntyre and S. A. Mason, unpublished results), had been performed. The wavelength used was 1.675 Å, and second-order beam contamination [expressed as $F^2(\lambda/2)/F^2(\lambda)$] was measured to be 2.3% ± 0.1%. The unit cell was determined from the centered angles of 55 reflections; the values found were $a = 27.332 \pm 0.008$ Å, $b = 32.158 \pm 0.012$ Å, $c = 34.274 \pm 0.007$ Å, $\alpha = 88.34° \pm 0.02°$, $\beta = 108.63° \pm 0.02°$, and $\gamma = 111.80° \pm 0.02°$.

To reduce the background due to incoherent scattering of hydrogen, the detector aperture was kept to a minimum, and scans were made with the $\omega$–$X\theta$ rather than the conventional $\omega$–$2\theta$ scan technique, i.e., the detector was moved so that the Bragg reflection stayed near the center of the detector. For the lowest angle data we used $\omega$–$\theta$ scans, changing gradually to $\omega$–$2\theta$ at the highest measurement angle of $2\theta = 60°$. As the detector aperture width was kept constant, at the higher

0006-2960/85/0424-5862$01.50/0 

angles the detector diaphragm obscured part of the diffracted beam. The intensities were corrected for this by a calibration curve based on strong reflections measured with larger apertures. The correction was linear with the Bragg angle and attained 8% at the highest value. In all, 7060 reflections including repeated test reflections were recorded over a span of 9 days. During this period no change was observed in the crystal scattering power as judged from measurements of selected strong reflections.

All reflections with $d$ spacings larger than 2.4 Å were recorded. In addition, the 70% strongest reflections with $d$ spacings between 2.4 and 2.0 Å—as judged from the previous neutron analysis of H-TLY—were measured. The step scan recorded reflections were reduced to structure factors (Lehmann & Larsen, 1974) and corrected for absorption by Gaussian integration and a calculated $\mu$ of 3.44 $cm^{-1}$. After averaging, there were 6103 reflections of which 6047 had nonzero intensities. These latter were used in the subsequent least-squares refinements.

*Ethanol Location and Structure Refinement.* The refinement program used throughout was the Hendrickson–Konnert constrained refinement program modified for neutron diffraction data (Wlodawer & Hendrickson, 1982). The starting parameters for the lysozyme molecule were the coordinates from the neutron diffraction study of the deuterated crystals, D-TLY (Mason et al., 1984). In the first series of refinements, only the protein was included in the model. The intermediate $R$ factor was 0.131. The ethanol molecules were then located by inspection of Fourier difference maps. Pairs of peaks at a distance of 2 Å or very elongated single peaks above noise level in the difference maps were identified as deuterated ethanol molecules if no peaks representing nitrate groups or disorder were found in the difference maps of H-TLY of the protein. As the ethanol molecule is likely to resemble the configuration of the water molecules that it replaces, it was in some cases not obvious whether the observed peaks represented a ethanol or a series of water molecules. Ethanol locations were therefore only assigned if the peaks in the H-TLY maps were small or did not resemble an ethanol molecule. At first, 15 possible ethanol sites were identified. As refinements proceeded simultaneously with the refinements of H-TLY and D-TLY, comparisons were made from time to time, and two suspect sites were eventually removed from the list. One was very near the possibly disordered Arg-45 and one corresponded to a nitrate group clearly visible in the D-TLY maps.

In the second series of refinements, ethanol molecules were included and were described as two hard spheres with radii 1 Å at an intercenter distance of 2 Å. The scattering factor of each sphere was given as

$$F(Q) = b \times 3(\sin Q - Q \cos Q)/Q^3$$

where $Q = 4\pi \sin\theta/\lambda$ and $b$ is the scattering length for a $CD_3$ group. Model calculations of scattering densities showed this description to be in good agreement with the scattering density of a $D_3C$–$CD_3$ molecule with elevated temperature parameters ($B$ = 50 Å$^2$). Similar model calculations showed that only highly ordered $H_2O$ groups would be observed, so no attempts were made to locate water molecules. Instead, the 16 best ordered water molecules from the D-TLY model were included, and in addition, four nitrate groups were found in the difference maps, in agreement with the difference maps for D-TLY and H-TLY.

No attempts were made to assign hydrogen and hydroxyl locations to the ethanol molecules on the basis of the scattering density. In Figure 1 are given three examples from difference

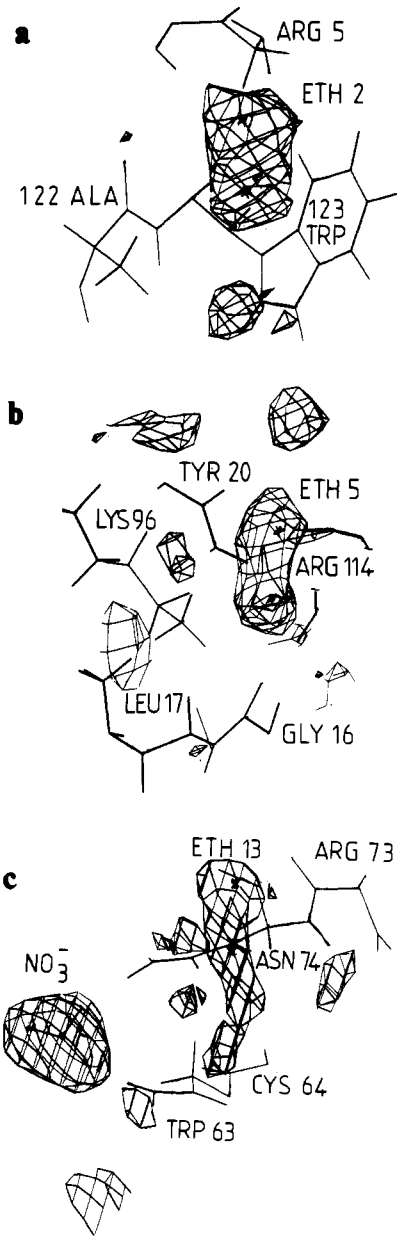


FIGURE 1: Examples of the observed shapes of ethanol molecules from difference maps. Only positive contours are given, and the maps are based on phases, which were calculated with only the lysozyme molecule. (a) A highly occupied site; (c) the (worst looking) lowest occupied site. Note the nitrate group in (c).

Fourier maps calculated after the last refinement, with use of phases from the lysozyme molecule only. In all cases, an elongated density is found, but there is no sign of lower density in the region where the O–H groups are placed. The size of the peaks for most of the ethanol molecules is in any case low compared to the main chain. The scattering density of an atom is given by

$$\rho(\vec{r}) \approx b/([(2\pi)^{3/2}u^3] \exp[-r^2/(2u^2)])$$

where $b$ is the scattering length, $B = 8\pi^2u^2$, and $r$ is the distance from the center of the atom. We get $\rho(o) \sim 1/B^{3/2}$, and consequently for a disordered ethanol group with $B \sim 50$ Å$^2$ compared with $B$ values in lysozyme around 11 Å$^2$, the ratio in peak height is $(11/50)^{3/2} = 1/10$. Including a further factor of $^1/_2$ because the difference map contains no phase information for the ethanols, we must then accept that the peak heights for ethanol at best will be between 5% and 10% of those for lysozyme, despite the impressive scattering power of a

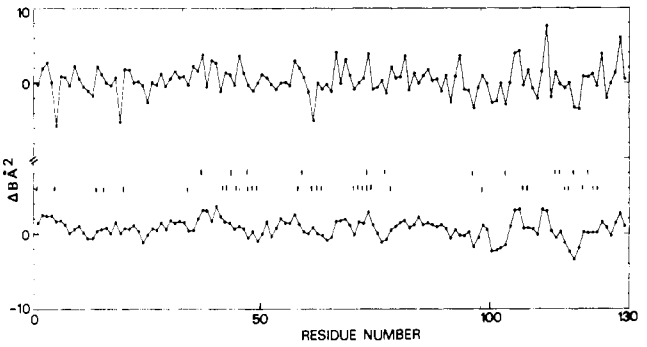


FIGURE 2: Difference between mean temperature factors $B$ (Å$^2$) for the ethanol data and for the H-TLY model. The lower curve is for the main-chain atoms, while the upper curve is for side-chain atoms. The locations where ethanol contacts occur are given as short vertical lines: the upper row is for hydrophilic contacts; the lower row is for hydrophobic contacts.

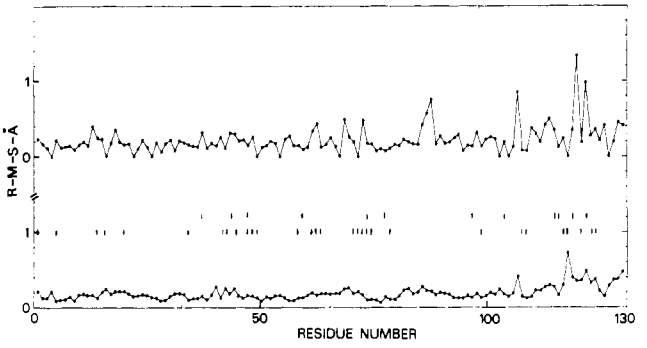


FIGURE 3: The rms positional difference between the final ethanol model and the starting parameters for the structural refinement (D-TLY model). The two curves and the vertical lines are defined as in Figure 2.

deuterated ethanol molecule. No attempts were therefore made to describe ethanol on an atomic level, although this might be possible later on chemical grounds.

A total of 13 ethanol sites were included in the refinements. In addition to structural and thermal parameters, the site occupation factors for all nonprotein species were varied; for the ethanol molecules, the final occupation factors ranged from 0.2 to 1.0.

*Inclusion of Disordered Solvent.* In an attempt to improve the agreement between observed and calculated low-order data, a description of the disordered, flat solvent was included in the structure factor equation. Details will be given elsewhere (Lehmann, 1985). The approach was to describe the solvent scattering as being equal in magnitude, but opposite in sign, to the scattering from a pseudomolecule. The pseudomolecule occupies the same molecular envelope as the protein molecule, but has the scattering density of the solvent. The molecular volume was simulated by hard spheres located at the atomic positions, and to obtain a smooth surface, it was convoluted with a sphere describing the average solvent molecule. The only variable parameter in this model is the solvent scattering density, $\rho_s$, which was varied in steps until a minimum was obtained in the agreement factors. The best results were obtained for $\rho_s = 0.0055 \times 10^{-12}$ cm/Å$^3$, corresponding to 20% ethanol (v/v) in the disordered solvent. This is less than the 25% in the mother liquor, but this is expected as there are undoubtedly solvent regions inside the crystal that are inaccessible to ethanol. The improvements in $R$ value arising from the solvent contribution were small. For the 1238 reflections with $d$ larger than 3.5 Å, the $R$ factor fell from 0.109 to 0.099. For all the data, the final $R$ factor was 0.097. After the final refinement, 491 out of 6778 bond distances deviated more than $2\sigma$ from ideality, where $\sigma$ for the distances involved ranged from 0.020 to 0.045 Å.

*Comparison with the Structure without Ethanol.* The main effect of the inclusion of solvent was to increase the value of the temperature parameters. The mean temperature parameter went from 8.8 to 11.3 Å$^2$ when the solvent was included, and this noticeably improved the agreement with the temperature factors for H-TLY, which were as well obtained by a refinement that included a solvent correction. We choose to compare with H-TLY, partly because the low scattering density of the $H_2O$ solvent would possibly lead to less biased temperature parameters than D-TLY and partly because the H-TLY and ethanol data were recorded at the same temperature. A comparison of temperature parameters is shown in Figure 2. The location of residues interacting with ethanol is given. The variations observed do not seem to correlate with the locations of the ethanol molecules. Further, the ethanol molecules do not seem to affect the general structure: final difference maps showed no indications of disorder beyond that observed in the structures not containing ethanol. A comparison between starting coordinates, i.e., the coordinates from D-TLY, and the final refined coordinates is given in Figure 3. Again, the location of residues interacting with ethanol is indicated. The mean difference in position comparing all atoms is 0.29 Å, and there is no indication of any strong variations along the chain.

Table I: Site Occupation, $Q$, and Temperature Factors, $B$ (Å$^2$), for Ethanol Groups[a]

| name | $Q$ | $B$ | feature in H-TLY |
|---|---|---|---|
| Eth 1 | 1.03 | 44 | strong peak in middle of ethanol |
| Eth 2 | 0.61 | 48 | nothing |
| Eth 3 | 0.32 | 41 | nothing |
| Eth 4 | 0.32 | 54 | nothing |
| Eth 5 | 0.28 | 12 | medium peak at one end of ethanol |
| Eth 6 | 0.25 | 46 | nothing |
| Eth 7 | 0.23 | 32 | medium peaks at both ends of ethanol |
| Eth 8 | 0.20 | 11 | medium peak at one end of ethanol |
| Eth 9 | 0.19 | 10 | strong peak at one end of ethanol |
| Eth 10 | 0.18 | 17 | nothing |
| Eth 11 | 0.18 | 29 | weak peak at one end of ethanol |
| Eth 12 | 0.16 | 32 | nothing |
| Eth 13 | 0.17 | 26 | nothing |

[a] The content of the corresponding region in H-TLY difference maps with phases from the protein only is given. A strong peak would normally indicate the location of a water molecule oxygen.

*Freezing Point Depression of Crystal Water.* During the diffraction experiment the cell dimensions and some selected reflections were monitored as a function of temperature. In normal triclinic lysozyme a well-defined phase change takes place at 257 ± 1 K (S. A. Mason, unpublished results). Below this point, the unit-cell volume decreases by 3.4% as the temperature is lowered slowly from 257 to 251 K. The structural basis for this transition is probably a freezing of the unbound water. For ethanol–lysozyme, the transition starts at a lower temperature, and the transition range is wider. Using as transition temperature the midpoint of this range, we get a temperature of 251 ± 1 K. Assuming normal solvent behavior, this freezing point depression would correspond to 17 ± 3% ethanol (v/v), which is in good agreement with the structural observations.

## Results and Discussion

Table I lists the site-occupation factors and thermal parameters for the 13 ethanol molecules. As the $CD_3$ groups are described by spheres of radius 1 Å, the convolution with thermal motion does not change the shape of the density substantially for the $B$ values obtained. Moreover, these values

Table II: Fractional Coordinates, $x$, $y$, and $z$, and Site Occupation Factors, $Q$, for the Bromoethanol Molecules Located by Yonath et al. (1978)[a]

| name | $x$ | $y$ | $z$ | $Q$ | ethanols |
|---|---|---|---|---|---|
| 1D | 0.756 | 0.881 | 0.367 | 0.10 | Eth 2 (1.1) |
| 2D | 0.667 | 0.591 | 0.914 | 1.00 | Eth 1 (2.0) |
| 3D | 0.216 | 0.736 | 0.892 | 0.15 | none |
| 4D | 0.754 | 0.464 | 0.294 | 0.10 | Eth 3 (3.5), Eth 7 (2.8) |
| 5D | 0.556 | 0.103 | 0.242 | 0.30 | none |

[a] The last column shows the corresponding ethanol molecules from the present study as well as the intermolecular distances (Å) in parentheses.

probably do not contain any physical information. Table I also contains a short comment on the density in the corresponding region of H-TLY. As discussed above, there is always a possibility that a well-ordered water structure mimics the density for an ethanol molecule, even when normal water is used, and even though the distance O–H···O is 2.75 Å compared to distances of 1.54 Å for C–C and 2.0 Å for the ethanol model used. In most cases, though, the density is low in the H-TLY map for the regions in question. It is worth noting that a very well bound water is observed at the site of Eth 1 both in H-TLY and in D-TLY, but because of the size of Eth 1 itself, there was no doubt that this is an ethanol. One possibility, which has not yet been explored for H-TLY and D-TLY, is that this water is in fact an acetate group. For $CH_3COO$, model calculations of density maps showed $CH_3$ to be nearly invisible, leaving a $D_2O$-like $CO_2$ group. Even then we would take the group to be an ethanol, as we could reasonably well assume for chemical reasons that $CD_3CD_2OH$ would replace $CH_3COOH$.

In all, the 13 sites gave a total of 4.1 molecules of ethanol, corresponding to 4% (v/v) of the solvent in the crystal. This is a comparatively small part of the available ethanol, but similar results have been obtained recently in other studies. For papain, where crystals were grown from 67% (v/v) methanol and where the structure was refined from X-ray data to a resolution of 1.65 Å (Kamphuis et al., 1984), only 26 out of 225 located solvent molecules could be regarded with any certainty as methanol. This corresponds to approximately 6% of the total solvent volume. Similarly from Crambin (Teeter, 1984), where crystals were obtained from 60% ethanol solutions, and which was refined from X-ray data to 0.945 Å and neutron data to 1.2 Å, only 7% of the solvent volume could be identified as ethanol.

*Comparison with Studies Using Bromoethanol.* Yonath et al. (1978) have already studied the interactions of triclinic lysozyme with bromoethanol. In their analysis, crystals were cross-linked (Yonath et al., 1977) so that a structure analysis could be carried out after a denaturation–renaturation cycle. For comparison with our work, the relevant analysis is that at the highest concentration, 0.75 M, before denaturation. Table II summarizes the coordinates and site occupation factors for the five locations given by Yonath et al., transformed to the unit-cell coordinate system of the present analysis. The transformation matrix was obtained by a least-squares fit between the sets of main-chain atoms for the two structures [coordinates for the lysozyme study of Yonath et al. were taken from the Protein Data Bank (Bernstein et al., 1977)]. The rms difference between the two sets of coordinates was 0.55 Å. In addition, Table II gives the corresponding ethanol molecules and the intermolecular distances.

In three out of the five sites, there is good agreement, and it is especially gratifying to note that 2D and Eth 1, which are the best located molecules for the two structures, coincide. For the two sites 3D and 5D, the ethanol difference maps were restudied. For the 5D location the map is empty. However, the 3D location is about 3 Å from a potential ethanol site, which was rejected in the very early stage of the analysis because it was near a few very well ordered water molecules observed in H-TLY. It is therefore possible that this site should after all have been included in the refinement. Altogether, the comparison shows that there is quite some resemblance in the protein binding nature for the two molecules, and therefore probably also in their denaturing action.

Table III: Intermolecular Contacts[a]

| name | contact |
|---|---|
| Eth 1 | Ile-58* m H (2.7), Asn-59 m H (2.9), Trp-63* s H (3.5), Ile-98* s H (2.7), Ala-107* s H (2.6), Trp-108* s H (3.6) |
| Eth 2 | Arg-5* s H (3.5), Ala-122* s H (3.2), Trp-123* s C (3.6) |
| Eth 3 | Arg-14* s H (3.1), Asn-37 s H (3.1), Arg-61* s H (2.8), Gly-71* s H (3.6) [Eth 7 (2.8)] |
| Eth 4 | Gln-41(*) m O (3.5), Ala-42* m H (3.4), Val-120* s H (3.5), Gln-121 s H (3.1) |
| Eth 5 | Gly-16* s H (3.0), Tyr-20* s H (3.1), Phe-34* s H (3.0), Lys-96 s H (2.5), Arg-114 s H (2.8) |
| Eth 6 | Trp-62* s H (2.9), Trp-63* s H (2.7), Asn-103 s O (3.3), Ala-107* s H (3.9) |
| Eth 7 | Arg-14* s H (3.3), Arg-61* s H (3.3), Trp-62* s H (2.9), Arg-73 s H (2.4) |
| Eth 8 | Arg-45* s H (2.9), Asn-77 m O (3.2), Ile-78* s H (1.8), Lys-116* s H (2.6), Gly-117* s H (2.6) [Eth 9 (2.0), Eth 10 (4.0)] |
| Eth 9 | Thr-43 m O (2.8), Asn-44* m H (2.2), Arg-45* m H (1.4) |
| Eth 10 | Cys-115 m O (3.8), Gly-117* m C (1.6), Thr-118 m H (2.2), Val-120* s H (3.6) |
| Eth 11 | Thr-47 m O (3.4), Asp-48* m C (3.7), Gly-49* s H (3.2), Pro-70* s H (3.4) [Eth 12 (3.6)] |
| Eth 12 | Thr-47* m H (3.2), Gly-49* s H (2.8) |
| Eth 13 | Lys-1* s H (3.7), Ser-72* s H (3.9), Arg-73* s H (3.2), Asn-74* s H (3.1) |

[a] An asterisk indicates that the contact is with hydrophobic parts, m means that the interaction is with the main chain, and s means that the interaction is with the side chain. Parentheses around the asterisk signify that the contact site is most probably hydrophobic. The atom type nearest the ethanol is indicated, and the distance (Å) is given in parentheses.

*Intermolecular Distances.* In order to get a picture of the typical interaction between the ethanol molecules and the lysozyme surface, interatomic distances were calculated. For ethanol, the two centers of the model molecule, located 2 Å apart, were used for the carbon atoms. For reasons given above, the ethanol oxygen and hydrogen atoms were not included in the calculation of interatomic distances, but they must be included in the estimate of the maximum possible contact length. The overwhelming majority of contacts are between hydrogen atoms in the two molecules, and in this case the distance between the ethanol carbon and the protein hydrogen atom would be 0.96 Å (carbon–hydrogen bond) plus twice the van der Waals radius of hydrogen, 2.4 Å (Pauling, 1960). The chosen maximum contact of 4 Å would therefore suffice to include all contacts of this kind. It is also long enough to accept contacts with carbon atoms on the protein as the van der Waals radius for carbon is around 1.7 Å (Pauling, 1960). For hydrogen bonds the limiting length was chosen to be 4 Å for the C(eth)–O–H···O(N) configuration, and this corresponds to an O···H contact of 2.2 Å, assuming a C(eth)–O–H angle of 120° and a linear hydrogen bond. A similar maximum O···H length was assumed for C(eth)–O···H bonds, and this gave a maximum inter atomic distance of 3.1 Å. As hydrogen bonds are seldom linear, this gives ample room for inclusion of all possible hydrogen bonds.

Table III summarizes the findings, and Figure 4 shows the local environments for the ethanol groups. On average, the

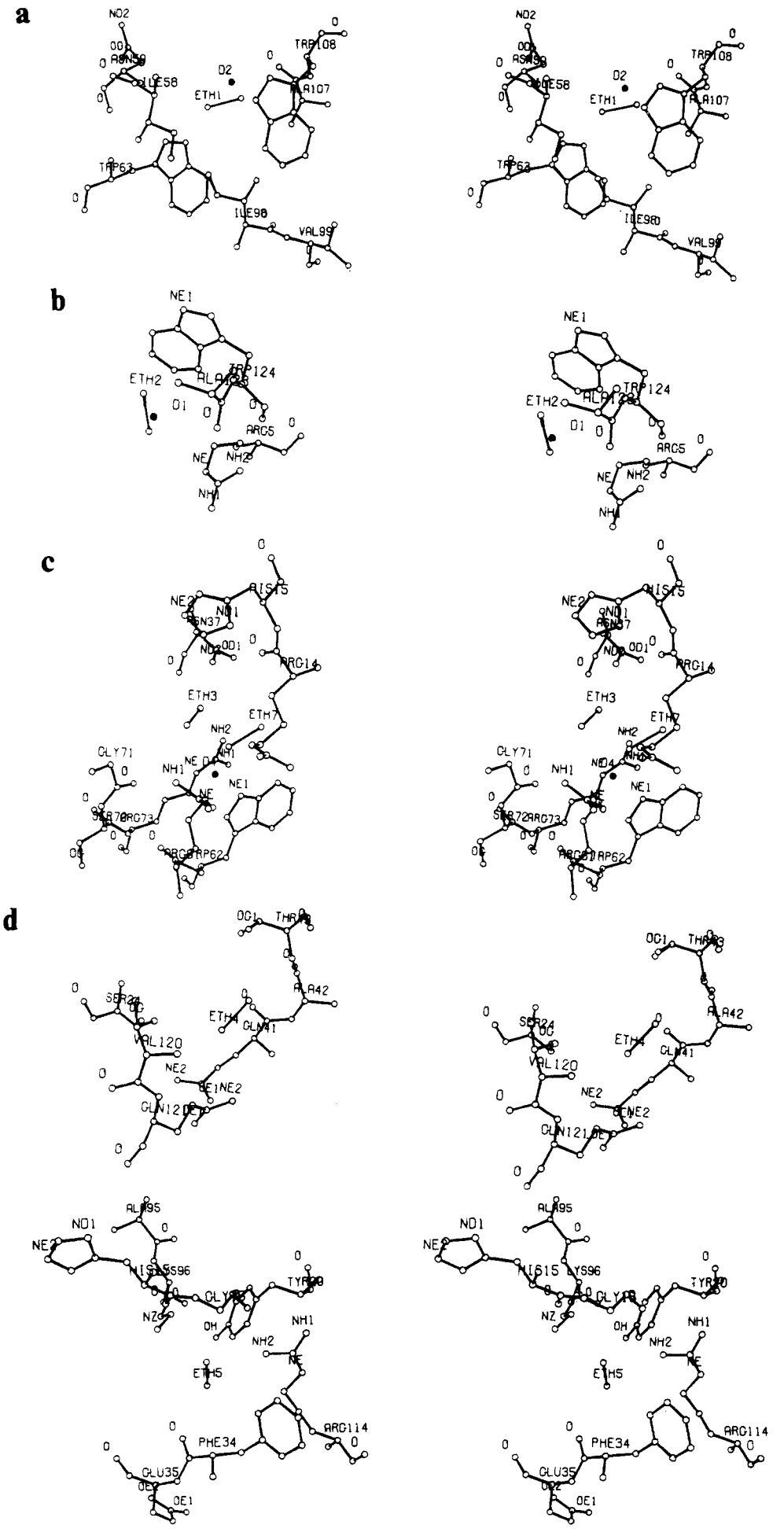
a
ND2
OD1
ASN58
ILE58
O2
ETH1
TRP108
ALA107
TRP63
ILE98
VAL99
b
NE1
ETH2
ALA128
TRP124
O1
ARG5
NE
NH2
NH1
c
HIS15
NE2
ND1
ASN37
OD1
ARG14
ETH3
ETH7
NH2
NH1
CLY71
NE O4
SER72
ARG73
ARG62
TRP62
d
OG1
THR43
ALA42
SER24
OG
ETH4
GLN41
VAL120
NE2
GLN121
OE1
e
ALA95
ND1
NE2
HIS15
LYS96
CLY98
TYR99
NZ
OH
NH1
NH2
NE
ETH5
PHE34
ARG114
GLU35
OE2
OE1

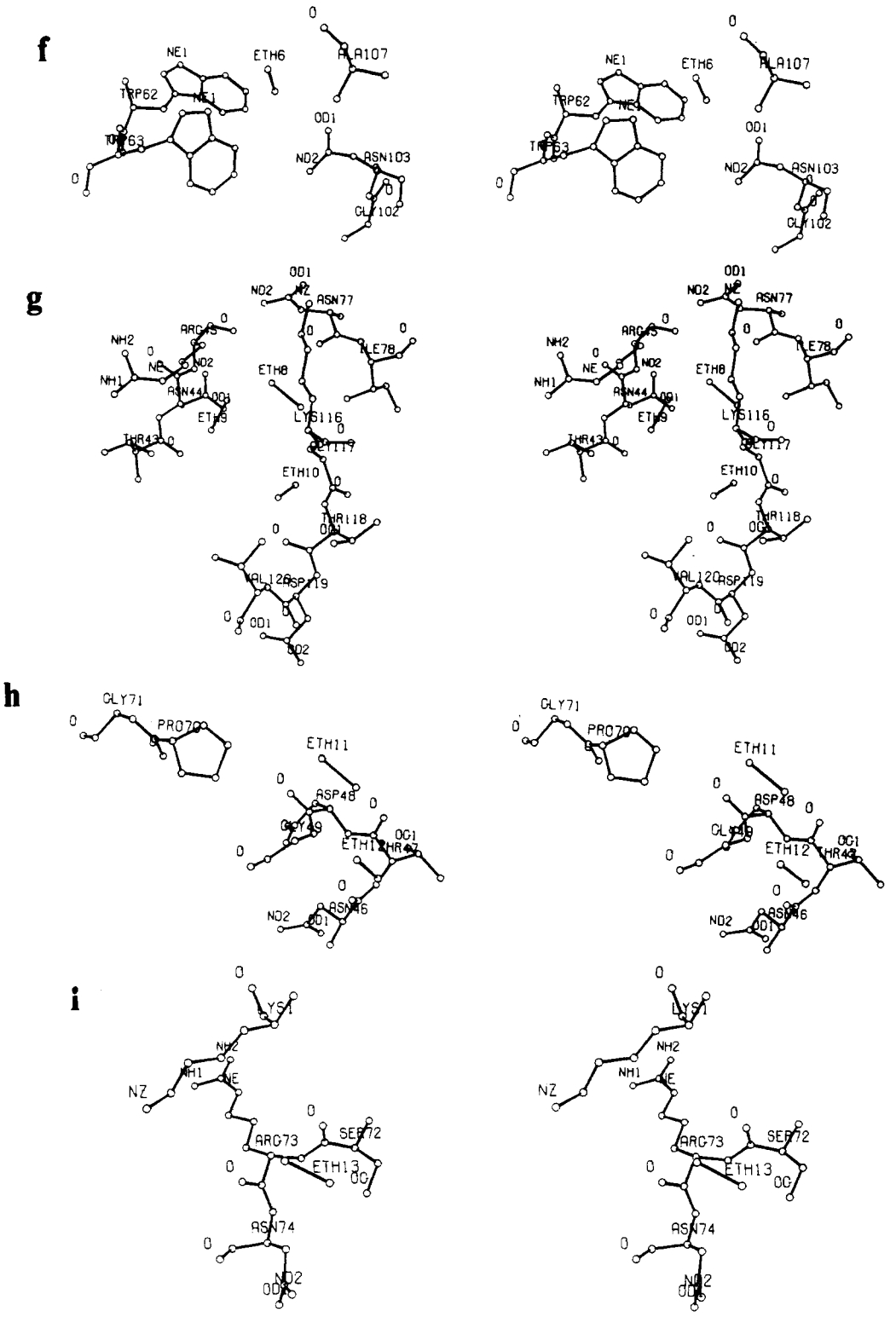


FIGURE 4: Stereo plots [using the program ORTEP, Johnson (1978)] for all the ethanols. Panels c, g, and h contain several ethanol molecules. In most plots, the residues given correspond to Table III. Cys-115 was removed from panel g for clarity, and a few residues are added here and there to improve comprehension. For Trp-62, which was assumed to be disordered in the refinement, only the site that is nearest ethanol is given, and this site is in any case the highest populated one. Dark points are the bromoethanol locations as determined by Yonath et al. (1978).

contact distance to hydrophobic hydrogen atoms is 3.1 Å. This is well below the limits mentioned above, and the value is undoubtedly partly governed by the van der Waals contact between the carbon atom of the ethanol group and the hydrogen atom, which was restrained to be a minimum of 3.05 Å in the least-squares refinement. It is however not unreasonably short. First, we should notice that the ethanol carbon atoms are at a distance of 2 Å rather than 1.54 Å, which will add to the true interatomic distance. Second, the ethanol hydrogen atoms are certainly not found on the line between the carbon and the lysozyme hydrogen atoms. Indeed, a realistic value for the van der Waals radius of a methyl group is 2.0 Å (Shrake & Rupley, 1973; Finney, 1975), which would give an average contact of 3.2 Å. Finally, keeping in mind that the ethanol groups are partially disordered, the most ordered part of the molecule will be found near the protein

and will thus shift the refined center of gravity in this direction.

In the hydrogen-bond contacts we see a strong distinction between the expected donor and acceptor configuration. In Table III, for C(eth)–O–H···O, we find 3.3 Å as mean value, while the C(eth)–O···H contacts are 2.7 Å on average. Both these values are in agreement with typical values for these kinds of arrangements.

One of the aims of this study was to look for structural evidence of ethanol association as the literature is nearly void of this kind of information (Beveridge et al., 1983). Three groups were found: Eth 3 + Eth 7, Eth 8 + Eth 9 + Eth 10, and Eth 11 + Eth 12. All the molecules have relatively low site-occupation factors, so from the diffraction study (which gives a time-averaged picture) we cannot decide whether ethanol molecules occur simultaneously in a certain region. Indeed, the minimum distance constraint in the structure refinement will prevent the molecules from overlapping. We might therefore suspect that the observed groups are representations of a multisite disorder for a single molecule. Even if the sites come from independent molecules, the probability for finding two uncorrelated molecules simultaneously is at best around 7%, i.e., the product of the two largest site occupation factors. Higher concentrations of alcohol and large site-occupations factors are therefore needed before we can discuss ethanol–ethanol interactions with any confidence.

*Ethanol–Lysozyme Interactions and the Denaturation Mechanism.* The interaction of ethanol with the lysozyme surface is best discussed by dividing the surface into two regions, one hydrophobic portion containing aliphatic and aromatic groups and a hydrophilic part consisting of polar and charged groups containing oxygen, nitrogen, or sulfur atoms.

For the interactions with hydrophilic groups, the hydrogen bonding is equally distributed between main-chain and side-chain locations, and likewise, there is an equal amount of hydrogen-bond donation and acceptance, as one might expect for an ethanol O–H group. In only one case, Eth 10, is there indication of the O–H being involved in both interactions simultaneously.

The interactions with hydrophobic sites in most cases involve the side-chain atoms, and most interactions are with the typical hydrophobic residues Ala, Trp, and Ile. A considerable amount of interaction is found as well with Arg and Lys, where the ethanol molecule is attached to the hydrophobic stem of the side chain.

The places where an interaction takes place are marked in Figures 2 and 3. The upper lines of markers indicate the position of interaction with hydrophilic sites, the lower line is for the hydrophobic interactions. Only the nearest contact as given in Table III is indicated. First, it should be noted that there is only a limited agreement between variations within the two plots. The reason for this could be that the rms positional deviations are calculated with respect to the starting parameters for the refinement, i.e., the D-TLY data, while the thermal motion differences relate to the compound that was measured at the same temperature, 280 K, and is thus most likely to have the same thermal behavior, namely, H-TLY. A good part of the variation is therefore likely to be noise from the other data. Beyond this there are however some relations between the locations of the ethanol molecules and the maximum fluctuations. The biggest fluctuations in both plots are in the residue ranges 35–45, 57–72, and 105–129, which do correspond to the major interaction sites for ethanol. One exception from this, though, is a peak in the rms plot around residue 87, for which there seems to be no explanation. Likewise, the locations of the ethanols were examined in the light of a surface accessibility calculation for the protein in the crystal [carried out by G. Bentley for D-TLY with the theory and programs of Lee & Richards (1971)]. The comparison showed that for a good part of the accessible areas no ethanol was found. It is most likely that for these locations ethanol, if present, is too disordered to given an observable signal.

Altogether, the specific interactions are mainly of hydrophobic nature. Of the 53 interactions given in Table III only 13 are hydrophilic, and the typical ethanol molecule is therefore 25% hydrophilic when interacting with lysozyme. We now assume that the hydrophilic activity is proportional to the area of the hydrophilic part of the surface, and we assume that for a given exposed atom its interacting surface is proportional to the square of its van der Waals radius. For ethanol, having five hydrophobic hydrogens, one hydrophilic hydrogen, and one oxygen, we then obtain a value for the hydrophilic nature of 34%. Another approach would be to assign a radius of 1.95 Å to the O–H, which is the mean of the van der Waals radius of oxygen, 1.5 Å, and of O–H, 2.4 Å. This gives 35% hydrophilicity. Finally, we could assign a van der Waals radius of 2 Å to the $CH_3$ end of ethanol, assume the surface of $CH_2OH$ to be divided into $^2/_3$ for $CH_2$, $^1/_6$ for C–O, and $^1/_6$ for C–O–H, and use 2.7 Å and 3.4 Å for the radii of C–O and C–O–H, respectively. In this case, we get 32% hydrophilicity. At first sight, the observed hydrophilic activity of 25% is therefore lower than that expected from a simple model for the ethanol molecule. However, as we do not know the water structure, some hydrophilic interactions are certainly missing. A reasonable minimum estimate would be to assume at least one interaction per ethanol, which adds three hydrophilic interactions and gives 29% observed hydrophilic nature. There is thus reasonable agreement between expectations and observations.

In their study on bromoethanol denaturation, Yonath et al. (1978) found indications of bromoethanol being hydrogen bonded to lysozyme, and they suggested that at higher concentrations further interactions between the hydrophobic portion of the small molecule and hydrophobic regions of the protein might occur. It would then be these interactions, involving the interior of the protein, that lead to significant unfolding. It is clear that once the protein is denatured, ethanol will interact with whatever part is exposed. Our observations do not however support the hypothesis that ethanol participates in the action of breaking up the molecule. Already at the stage well below denaturation, we find that the ethanols are satisfactorily bound, so we have no reason to suspect any changes in the observed ethanol–lysozyme structure as more ethanol is added. The major effect would be to increase the occupation factors of the sites where ethanol is already bound and to add further sites. As the latter will have lower binding constants (i.e., not being observable in the present study), it is unlikely that they can have any important effect on the lysozyme structure.

Lee & Richards (1971) and Shrake & Rupley (1973) have estimated that the surface of lysozyme consists of between 41% and 53% apolar residues. All of this surface can probably not be reached by ethanol molecules, and only part of the ethanol surface—about 65%—is hydrophobic. We can therefore not determine precisely the point where the surface saturation occurs. At this stage, however (probably above 50% ethanol), the content of ethanol in the water near the surface will be lower than that in the bulk solution, the water will redistribute, and the protein will dehydrate, leading to conformational rearrangements. Such changes have been observed by Ham-

aguchi & Kurono (1963) for ethanol volume concentrations around 60%.

An important requirement for conformational stability is the fulfilment of hydrogen bonding, as the penalty in energy for leaving a potential hydrogen-bond donor/acceptor unsatisfied is high. When water is removed from the protein, it is easier to replace hydrogen-bond configurations on the side chains than on the main chain, both because there is more space around the side chains and because these are more flexible. One key factor in stabilizing the native fold is therefore undoubtedly the water molecules bound to the main chain. When they are removed, intramolecular binding among the peptide units can become necessary, and helical structure is promoted. In agreement with this, helical structure persists for lysozyme even at high alcohol concentrations (Hamaguchi & Kurono, 1963). Indeed, promotion of helical structure seems to be a common aspect of denaturation by alcohols [see, e.g., p 303 of Lapanje (1978)].

Although our measurements are concerned only with the structure of lysozyme in its native state, the nature of the ethanol binding therefore suggests that a main step in a conformational change of the protein by high alcohol concentration is a dehydration of the molecule, followed by promotion of helical structure and binding of ethanol to the newly exposed residues. The point of transition might occur when the capacity of the surface for bonding of the molecule in question is exhausted and should be tractable by surface accessibility calculations.

## Conclusions

The present study was undertaken in order to determine the mode of binding of ethanol to the protein lysozyme. From 13 possible locations of ethanol on the lysozyme surface we have determined that the ratio of hydrophilic to hydrophobic affinity is in agreement with the expected nature of ethanol binding. We find as well that at 25% (v/v) ethanol concentration the ethanol binding does not influence significantly either the structure or the motion of lysozyme. We are therefore led to conclude that ethanol denaturation is not likely to occur by direct interaction of ethanol with the interior part of the lysozyme molecule but might proceed via a destruction of the water structure, especially near the main chain of the protein. The result of this would be a dehydration of the macromolecule followed possibly by an increase in helix formation.

The study was also undertaken to test the applicability of neutron diffraction for the study of small molecule interactions with proteins. With suitable choice of deuteration of the constituents, the probe molecule should be visible, even in case of considerable disorder. The outcome of the analysis shows this to be the case, and although the crystal size required is larger than that for X-ray analysis, with modern neutron diffraction techniques many systems can be studied.

## Acknowledgments

We thank Dr. F. K. Larsen for preliminary test measurements carried out at Risø National Laboratories, Denmark. We are indebted to members of the Laboratory of Molecular Biophysics at the Department of Zoology, Oxford University, the protein group at CNRS, Luminy Campus, Marseille, and the biostructural group of the Wallenberg Laboratory of the University of Uppsala for use of their graphics systems and for much advice and help.

## References

Allibon, J. R., Filhol, A., Lehmann, M. S., Mason, S. A., & Simms, P. *J. Appl. Crystallogr.* (1981) *14*, 326–328.

Bernstein, F. C., Koetzle, T. F., Williams, G. J. B., Meyer, E. F., Jr., Brice, M. D., Rodgers, J. R., Kennard, O., Shimanouchi, T., & Tasumi, M. (1977) *J. Mol. Biol. 112*, 535–542.

Beveridge, D. L., Ravishanker, G., & Mezei, M. (1983) *Structure and Dynamics: Nucleic Acids and Proteins* (Clementi, E., & Sarma, R. H., Eds.) pp 477–483, Adenine Press, Guilderland, NY.

Finney, J. L. (1975) *J. Mol. Biol. 96*, 721–732.

Hamaguchi, K., & Kurono, A. (1963a) *J. Biochem. (Tokyo) 54*, 111–122.

Hamaguchi, K., & Kurono, A. (1963b) *J. Biochem. (Tokyo) 54*, 497–505.

Hodsdon, J. M., Sieker, L. C., & Jensen, L. H. (1975) *ACA Abstr. 3*, 16.

Johnson, C. K. (1978) *ORTEP II*, Report ORNL-5138, Oak Ridge National Laboratory, Oak Ridge, TN.

Kamphuis, I. G., Kalk, K. H., Swaite, M. B. A., & Drenth, J. (1984) *J. Mol. Biol. 179*, 233–256.

Koester, L., & Rauch, H. (1981) *Summary of Neutron Scattering Lengths*, IAEA-Contract 2517/RB, International Atomic Energy Agency, Vienna.

Lapanje, S. (1978) *Physicochemical Aspects of Protein Denaturation*, Wiley, New York.

Lee, B., & Richards, F. M. (1971) *J. Mol. Biol. 55*, 379–400.

Lehmann, M. S. (1985) Report 85LEIIT, Institut Laue-Langevin.

Lehmann, M. S., & Larsen, F. K. (1974) *Acta Crystallogr., Sect. A: Cryst. Phys., Diffr., Theor. Gen. Crystallogr. A30*, 580–584.

Lehmann, M. S., & Zaccaï, G. (1982) *Biophysics of Water* (Franks, F., & Mathias, S., Eds.) pp 134–136, Wiley, New York.

Mason, S. A., Bentley, G. A., & McIntyre, G. J. (1984) *Neutrons in Biology* (Schoenborn, B. P., Ed.) pp 323–334, Plenum Press, New York.

Pauling, L. (1960) *The Nature of the Chemical Bond*, 3rd ed., Cornell University Press, Ithaca, NY.

Shrake, A., & Rupley, J. A. (1973) *J. Mol. Biol. 79*, 351–371.

Teeter, M. M. (1984) *Proc. Natl. Acad. Sci. U.S.A. 81*, 6014–6018.

Wlodawer, A., & Hendrickson, W. A. (1982) *Acta Crystallogr., Sect. A: Found. Crystallogr. A38* 239–247.

Yonath, A., Sielecki, A., Podjarny, A., Moult, J., & Traub, W. (1977) *Biochemistry 16*, 1413–1417.

Yonath, A., Podjarny, A., Honig, B., Traub, W., Sielecki, A., Herzberg, O., & Moult, J. (1978) *Biophys. Struct. Mech. 4*, 27–36.